

KAUNAS UNIVERSITY OF TECHNOLOGY

NERITA ŽMUIDZINAVIČIENĖ

**Influence of Te(VI) on electrodeposition of manganese coatings**

Summary of Doctoral Dissertation  
Physical Sciences, Chemistry (03P)

2015, Kaunas

The research was carried out during 2010–2015 at Kaunas University of Technology, Department of Physical and Inorganic Chemistry.

**Scientific supervisor:**

Prof. Dr. Algirdas ŠULČIUS (Kaunas University of Technology, Physical Sciences, Chemistry – 03P).

**Lithuanian language editor:**

Jurgita MIKELIONIENĖ

**English Language editor:**

Tony BEXON

**Dissertation Defense Board of Chemical Science Field:**

Prof. Dr. Habil. Algirdas ŠAČKUS (Kaunas University of Technology, Physical Sciences, Chemistry – 03P) – **chairman**;

Doc. Dr. Nijolė DUKŠTIENĖ (Kaunas University of Technology, Physical Sciences, Chemistry – 03P);

Prof. Dr. Habil. Aivaras KAREIVA (Vilnius University, Physical Sciences, Chemistry – 03P);

Prof. Dr. Habil. Rimantas RAMANAUSKAS (Center for Physical Sciences and Technology, Institute of Chemistry, Physical Sciences, Chemistry – 03P);

Prof. Dr. Eugenijus VALATKA (Kaunas University of Technology, Physical Sciences, Chemistry – 03P).

The official defense of the dissertation will be held at the open meeting of the Board of Chemical Science field at 10 a.m. on December 21, 2015 in the Rectorate Hall at the Central Building of Kaunas University of Technology.

Address: K. Donelaičio st. 73-403, LT-44249, Kaunas, Lithuania.

Phone (370) 37 300042, fax (370) 37 324144, e-mail [doktorantura@ktu.lt](mailto:doktorantura@ktu.lt)

Summary of doctoral dissertation was sent on 20 november, 2015

The Dissertation is available at <http://ktu.edu> and at the library of Kaunas University of Technology (K. Donelaičio st. 20, Kaunas).

KAUNO TECHNOLOGIJOS UNIVERSITETAS

NERITA ŽMUIDZINAVIČIENĖ

**Te(VI) įtaka mangano dangų elektrolitiniam  
nusodinimui**

Daktaro disertacijos santrauka  
Fiziniai mokslai, chemija (03P)

2015, Kaunas

Disertacija rengta 2010–2015 metais Kauno technologijos universitete, Fizikinės ir neorganinės chemijos katedroje. Mokslinius tyrimus rėmė Lietuvos mokslo taryba.

**Mokslinis vadovas:**

Prof. dr. Algirdas ŠULČIUS (Kauno technologijos universitetas, fiziniai mokslai, chemija – 03P);

**Anglų kalbos redaktorius:**

Tony BEXON

**Lietuvių kalbos redaktorė:**

Jurgita MIKELIONIENĖ

**Chemijos mokslo krypties disertacijos gynimo taryba:**

Prof. habil. dr. Algirdas ŠAČKUS (Kauno technologijos universitetas, fiziniai mokslai, chemija, 03P) –**pirmininkas**;

Doc. dr. Nijolė DUKŠTIENĖ (Kauno technologijos universitetas, fiziniai mokslai, chemija – 03P);

Prof. habil. dr. Aivaras KAREIVA (Vilniaus universitetas, fiziniai mokslai, chemija – 03P );

Prof. habil. dr. Rimantas RAMANAUSKAS(Fizinių ir technologijos mokslų centras, Chemijos institutas, fiziniai mokslai, chemija – 03P );

Prof. dr. Eugenijus VALATKA (Kauno technologijos universitetas, fiziniai mokslai, chemija – 03P).

Disertacija bus ginama viešajame chemijos mokslo krypties tarybos posėdyje, kuris įvyks 2015 m. gruodžio 21 d. 10 val. Kauno technologijos universiteto Centrinė rūmų Rektorato salėje.

Adresas: K. Donelaičio g. 73-403, LT-44249, Kaunas, Lietuva.

Tel. (370) 37 300042, faksas (370) 37 324144, el. p. [doktorantura@ktu.lt](mailto:doktorantura@ktu.lt)

Disertacijos santrauka išsiųsta 2015 m. lapkričio 20d.

Su disertacija galima susipažinti interneto svetainėje <http://ktu.edu> ir Kauno technologijos universiteto bibliotekoje (K. Donelaičio g. 20, Kaunas).

## INTRODUCTION

### **Relevance of the work.**

Coatings of different metals are used for the cathodic protection of steel. Manganese, which corrodes in neutral and alkaline media, forms a layer of insoluble corrosion products and this layer decreases further corrosion of this metal. Mn electrodeposits are perfectly suitable as sacrificial coatings for protecting ferrous substrates against corrosion. In some media, even in the case of porous and rough coating, manganese protects steel against corrosion better than zinc.

The electrodeposition process of manganese coatings is positively affected by inorganic compounds of S, Se, and Te dissolved in an ammonium sulphate bath as additives. The literature data on the influence of microhardness and internal stress of some electrodeposited metals on corrosion properties of these coatings are limited. It should be noted that Mn, electrodeposited from an ammonium sulphate bath without an additive, is characterized by tensile stresses. In the literature, only fragmentary data on the Mn, electrodeposited from different composition manganese electrolytes containing S and Se additives, microhardness, and influence of some metal ions ( $Zn^{2+}$ ,  $Cd^{2+}$  and  $Cu^{2+}$ ) impurities on the microhardness of electrodeposited Mn coatings can be found. It is known, that the quality of coatings for the metals and alloys and their adhesion to substrate are determined by the internal stresses. Compression stresses of coatings can cause the coating delamination from the substrate, and the tensile stresses can cause cracks of coatings. Literature data on the influence of Te compounds as additives in the electrolytic bath on microhardness and internal stresses of Mn coatings are rather sparse.

Therefore, from theoretical and practical points of view, it is relevant to determine the influence of Te compounds as additives on the physical and mechanical properties of electrolytic Mn deposition coatings, and which condition the corrosion properties of these coatings.

The present work is a continuation of the research on Mn and its alloys in the electrochemistry field carried out at the Department of Physical and Inorganic Chemistry, Kaunas University of Technology and is devoted to the electrodeposition of Mn coatings and their characterisation.

### **Aim of the work.**

To determine the influence of a Te(VI) additive in a manganese ammonium sulphate bath on electrodeposition of electrolytic Mn coatings and the physical-mechanical properties of electrodeposited coatings. In addition to investigating the possibility of application of electrodeposited Mn coatings with Te intermixtures for the protection of steel against corrosion.

In order to reach the aim of the work, the following goals had to be completed:

1. To electrodeposit Mn coatings from the stableacidic manganese ammonium sulphate bath of optimal concentration with the Te(VI) additive at low concentration, and investigate their chemical and phase composition, current efficiency, coating morphology, physical-mechanical properties, and resistance towards corrosion.

2. To investigate the influence of concentration of the Te(VI) additive (0.55–2.20 mmol/l) and temperature on the electrodeposition process of Mn coatings and cathode polarization in the acidic manganese ammonium sulphate bath.

3. To investigate the resistance towards corrosion of electrolytic Mn coatings and evaluate the influence of phosphatic coatings on the increased resistance.

#### **Scientific novelty of the work.**

1. Optimal electrolysis conditions, enabling electrodeposition of high quality, nanocrystal size and resistant towards corrosion electrolytic Mn coatings containing Te from an acidic manganese ammonium sulphate bath have been determined. It has been shown that phosphatic coatings increase significantly the resistance against corrosion of electrolytic Mn coatings with Te additive.

2. The influence of the bath temperature and current density on morphology, size of crystalites, internal stresses and microhardness of electrolytic Mn coatings electrodeposited from MASB with Te(VI) additive has been determined.

3. It has been determined, that electrolytic Mn coatings electrodeposited from a manganese ammonium sulphate bath are nanocrystal, and an average size of crystalites and variation of Te concentration in the pits and bumps on the coating surface depend on the current density and electrolyte temperature.

#### **Practical value of the work.**

Nanocrystal electrolytic Mn coatings with Te additive, electrodeposited under optimal electrolysis conditions (2.20 mmol/l Te(VI) additive concentration, current density 15 A/dm<sup>2</sup>) from an acidic manganese ammonium sulphate bath, can be used for protection of steel against corrosion.

**Approval and publication of research results.** Results of the research are presented in 8 publications: 3 of them have been published in journals included into the Institute for Scientific Information (ISI) database; 2 papers have been published in the journal “Chemical Technology”, and 3 are proceedings of conferences.

**Structure and content of the dissertation.** The dissertation consists of an introduction, literature review, experimental part, results and discussion, conclusions, the lists of references and publications on the dissertation topic. The list of references includes 128 bibliographic sources. The main results are discussed on 87 pages, illustrated in 48 figures and 18 tables.

**Statements presented for the defense:**

1. Elemental Te formed on the cathode surface in the acidic electrolyte depolarizes cathodic process and determines further origination of higher value limit current at the potential interval from -1.1 V to -1.3 V. It has been proven that separate MnTe crystallites are formed on the surface of carbon steel cathode at this potential interval.

2. Electrolytic Mn coatings electrodeposited from a manganese ammonium sulphate bath are nanocrystal, whereas concentration of Mn and Te present in the pits and bumps of the coating surface depends on the electrolysis conditions.

3. Electrolytic Mn coatings with Te additive electrodeposited at  $15 \text{ A}\cdot\text{dm}^{-2}$  are resistant towards corrosion. The resistivity towards corrosion of Mn coatings with Te additive is increased by means of phosphatic coatings.

## EXPERIMENTAL

All reagents used in the experiments were at least of analytical reagent quality.

### Materials

A stable manganese ammonium sulphate bath (MASB) was used: 0.95 M  $(\text{NH}_4)_2\text{SO}_4$ , 0.62 M  $\text{MnSO}_4\cdot 5\text{H}_2\text{O}$ . Sodium tellurate  $\text{Na}_2\text{TeO}_4\cdot 2\text{H}_2\text{O}$  (or  $\text{Na}_2\text{H}_4\text{TeO}_6$ ) was used as an additive of Te(VI) in the MASB. The pH of the obtained stable electrolyte was adjusted by solutions of concentrated  $\text{NH}_3\cdot\text{H}_2\text{O}$  and  $\text{H}_2\text{SO}_4$  (1:1). The pH of electrolytes and other solutions was measured with the pH-meter WTW330 (Portugal). The electrolyte was not stirred.

The surfaces of the electrodes were polished with a felt wheel by using polishing paste, degreased by Vienna lime and dipped into a 2 % solution of sulphuric acid. All chemicals were analytically pure grade (Aldrich and Reakhim, Russia). Twice-distilled water was used in the preparation of the solutions. Measurements were made at  $20\pm 1^\circ\text{C}$ .

Mild carbon steel (St-3, Russia) plates, size  $20\times 20 \text{ mm}$ , were used as cathodes. Pb-1%Ag alloy plates coated with a  $\text{MnO}_2$  film were used as inert anodes. Such anodes are widely used for electrodeposition of Mn and its alloy (Ni-Mn, Zn-Mn) coatings in industry. They were produced by alloying Pb with Ag and subsequent anodic pretreatment in manganese-ammonium sulphate electrolyte with a small amount of  $\text{NH}_4\text{Br}$  additive. PVC fabric diaphragms were used for separating cathodic and anodic compartments of the electrodeposition cell. A constant amount of charge ( $2 \text{ A h dm}^{-2}$ ) was used in all electrodeposition experiments. The polarization curves were recorded at potential sweep rates of  $5\text{--}30 \text{ mV s}^{-1}$ . The reference electrode was saturated Ag/AgCl and the cathode was a square mild carbon steel plate (St-3, Russia) with a working area of  $100 \text{ mm}^2$ . The non-working surface of the electrodes was covered with organic glass.

Investigation of concentrations of Te and Mn in coatings was carried out by an atomic absorption spectroscopy (AAS-PERKIN ELMER 503). For detecting

Mn and Te concentrations in coatings, they were dissolved in a minimal volume of HNO<sub>3</sub> (1:4) solution and made up to the volume of the diluted 1 % HCl.

The XPS spectra of Mn coatings were recorded on a Kratos XSAM800 spectrometer (radiation Al K $\alpha$  – 1468.6 eV). Vacuum in the analysing chamber was kept at a level of 10<sup>-6</sup> Pa, and the distribution of elements in the depth was determined by sputtering with an Ar<sup>+</sup> gun with the ion energy of about 1.0 keV, current density and duration of etching were 50  $\mu\text{A}\cdot\text{cm}^{-2}$  and 10 min. The maximum accuracy of the method was 0.1 at. %.

The structure of electrodeposits was investigated by X-ray diffraction analysis (XRD) using a Bruker D8 Advance diffractometer. In accordance with the X-ray data, the diffraction patterns of Mn coatings were identified using Bruker AXS software (program EVA), and a PDF-2 database. The calculation of crystallite size was performed in a conventional way according to the Scherrer formula after the measurements of the full widths at the half maxima of the peaks in the X-ray diffractograms using the computer program X-fit. The reliability of the method reached 98 %.

Profile of the relative concentration of surface components was obtained using a glow discharge spectrometer (GDS - Leco, Model 850A). The structure of electrodeposits was investigated by XRD using a Bruker diffractometer (Model D8 Advance), morphology and detailed elemental analysis of the surface of the electrodeposits were investigated using a scanning electron microscope (SEM) with an energy-dispersive X-ray (EDX) spectra analyser (Jeol Model DSM-5400LV).

The morphology of electrodeposits was investigated by an atomic force microscopy (AFM) with the microscope NT 206 (Belarus), by scanning a surface area of 12 $\times$ 12  $\mu\text{m}$  of a sample in air using the contact mode. The investigation of morphology of the surface of the electrodeposits was performed using a FEI Qanta 200 FEG scanning electron microscope (SEM) with a Bruker XFlash<sup>®</sup> 4030 detector for high resolution energy dispersive X-ray (EDX) spectroscopy.

Microhardness (HV) of Mn coatings was measured by the Vickers method using an optical microscope PMT-3 (Russia) equipped with a graduated ocular MOB-1-15<sup>x</sup>. The graduation value of the ocular was 3.125 $\cdot$ 10<sup>-4</sup> mm (object-glass F-6.2(0.65)). The applied load was 0.49 N. The mean value of HV was estimated from 15 measurements carried out in the central area of the coated electrode. Tensions developed during electrodeposition were measured by the cathode-bending method. The mechanical support of the electrode was a copper slab (100 mm  $\times$  10 mm  $\times$  0.3 mm). The active cathode area was 1000 mm<sup>2</sup>, the rest of the surface of copper slab was coated with pure paraffin. The bending of the free end of the slab was measured with an optical microscope PMT-3 (Russia) equipped with a graduated ocular MOB-1-15<sup>x</sup>. The graduation value of ocular was 1.175 $\cdot$ 10<sup>-3</sup> mm (object-glass F-23.2(0.17)). Tensions of coatings  $\sigma$  were calculated according to the Barklic-Davies formula:



$$\sigma = \frac{E_{Cu} \cdot d_1^2 \cdot z}{3d_2 \cdot l^2}$$

where  $E_{Cu}$  is Young's modulus of cathode material ( $E_{Cu} = 108\,000$  MPa);  $d_1$  and  $d_2$  (mm) are the thickness of the cathode and coating, respectively;  $l$  (mm) is the length of the cathode;  $z$  (mm) is the cathode bending from the initial position. Mean values and 95 % confidence intervals were computed from sets of four measurements.

## RESULTS AND DISCUSSION

### 2.1. Electro depositions of Mn coatings at room temperature.

#### 2.1.1. Cathode polarization

Potentiodynamic measurements in the MASB without additive at different potential sweep rates are shown in Fig. 1. Maximal limiting current density  $j_{max}$  in the potential range from  $-0.8$  V to  $-1.0$  V (vs. Ag/AgCl) was observed. Electrochemical discharge of hydrogen on the steel electrode takes place at this potential range. It is known that  $NH_4^+$  ions participate in this process as well:

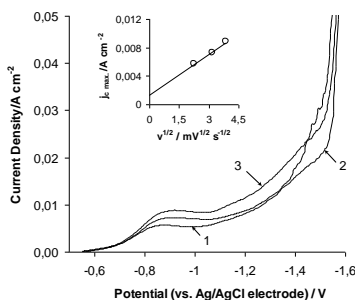
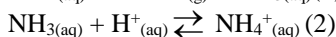
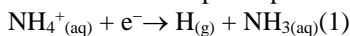


**Fig. 1.** Steel cathode polarization in MASB without additive at different potential sweep rates: **1** –  $5$   $mV\ s^{-1}$ ; **2** –  $10$   $mV\ s^{-1}$ ; **3**–  $15$   $mV\ s^{-1}$ . Dependence of maximal limiting current density  $j_{max}$  (at potential  $-0.9$  V) on the square root of potential sweep rate  $v^{1/2}$  is presented in insertion

The limiting current density for the discharge of  $H^+$  ions increased as well (Fig. 1 insertion) when the sweep rate of cathode potential was increased. A linear dependence of the maximal limiting current density  $j_{max}$  on the square root of the sweep rate  $v^{1/2}$ , which almost passes through the origin, suggests that the

electrochemical reduction of  $H^+$  ions is limited by restricted diffusion of these ions to the cathode surface.

In the meantime, the maximal limiting current density  $j_{\max}$  in the MASB grows with the increasing of Te(VI) additive concentration in this potential range (Fig. 2).

Changing the potential sweep rate in the MASB with 2.20 mM of Te(VI) additive leads to the growth of the maximal limiting current density  $j_{\max}$  (Fig. 3). It was detected that at any concentration of Te(VI) in the MASB; the  $j_{\max} = f[v^{1/2}]$  does not pass through the origin. The value of maximal limiting current density  $j_{\max}$  is about 1.5 times greater than the one with the absence of Te(VI) additive (Fig. 3 insertion).

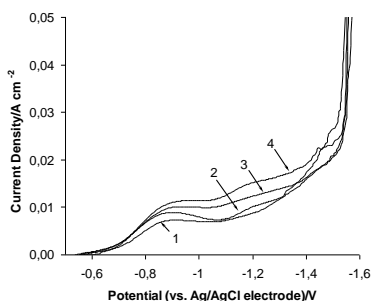


**Fig. 2.** Influence of Te(VI) additive concentration on the polarization of steel cathode in MASB at a potential sweep rate  $10 \text{ mV s}^{-1}$ : 1 – 0 mM (without additive); 2 – 0.55 mM; 3 – 1.10 mM; 4 – 2.20 mM

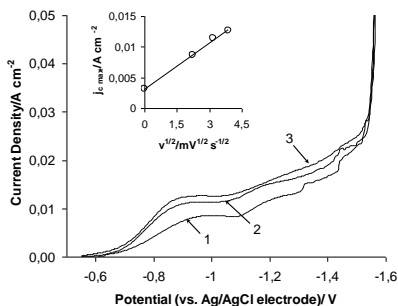
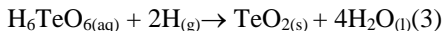
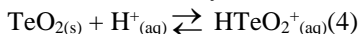


**Fig. 3.** Steel cathode polarization in MASB with 2.20 mM additive at different potential sweep rates: 1 –  $5 \text{ mV s}^{-1}$ ; 2 –  $10 \text{ mV s}^{-1}$ ; 3 –  $15 \text{ mV s}^{-1}$ . Dependence of maximal limiting current density  $j_{\max}$  (at potential  $-0.9 \text{ V}$ ) on the square root of potential sweep rate  $v^{1/2}$  is presented in insertion

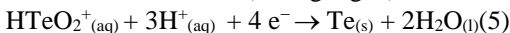
This suggests that in the potential range from  $-0.8$  V to  $-1.0$  V (vs. Ag/AgCl) the diffusion process was not limited and mixed processes took place. It had been presumed, that the electrochemical reduction of  $H^+$  ions, electrochemical and chemical Te(VI) reduction to Te(IV) and elemental Te took place on the surface of the steel cathode. Atomic hydrogen (reaction 1) as a very active reducing agent may take part in the reduction of orthotelluric acid  $H_6TeO_6$  to tellurium(IV) oxide:



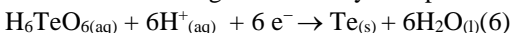
Since, a MASB is strongly acidic, at the initial moment of electrolysis protonized tellurium(IV) oxide  $HTeO_2^+$  may be formed near the cathode surface:



This particle can be easily formed by electrochemical reduction when the electrode potential is less than  $-0.77$  V (vs. Ag/AgCl):



It is known that in this potential range in a strongly acidic medium and in the presence of ammonium the following reaction may take place:



Tellurium formed on the cathode surface depolarized process and lead to the larger limiting current density in the potential range from  $-1.0$  V to  $-1.3$  V (vs. Ag/AgCl). It is presumed that the complex reduction process took place by forming manganese telluride MnTe, which had a positive influence on further electrodeposition of manganese coating.

The above mentioned assumptions were supported by 1 h electrolysis experiments in the MASB with 2.20 mM of Te(VI) additive under potentiostatic conditions at  $-1.0$  V and  $-1.3$  V (vs. Ag/AgCl). SEM and EDX analysis of the carbon steel cathode surface have shown that separate crystallites of MnTe start forming at these potentials. The formation of this compound confirms very well the ratio of atomic concentrations of detected Mn and Te on the cathode surface (Fig.4). It had been presumed, that Te and its compounds, similar to the Se and its compounds, passivated the cathode surface and decreased the corrosion rate of electrodeposited manganese coating in a strong acidic MASB.

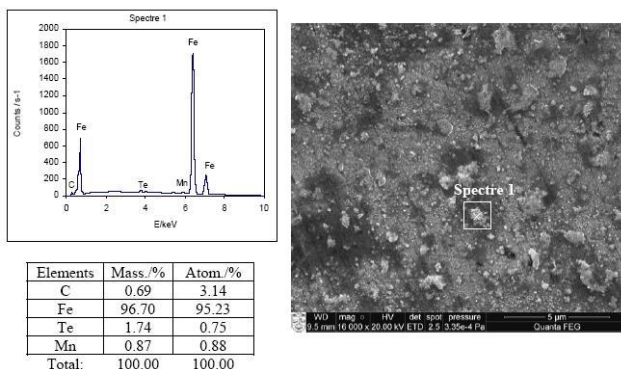


**Fig. 4.** Elemental composition of deposit determined by SEM with elemental EDS analyser. Deposit was electrodeposited from MASB with 2.20 mM of Te(VI) additive under potentiostatic conditions at  $-1.0$  V (vs. Ag/AgCl)

### 2.1.2. Chemical composition and current efficiency

Manganese coatings were not obtained from the MASB without Te(VI) additive at  $\text{pH} = 2.3$ . An electrodeposited manganese coating corroded in the MASB during electrolysis and only hydrogen evolution was observed in the investigated cathode potential range. When the current density in the MASB with 2.20 mM Te(VI) additive increased from 2 to  $15 \text{ A}\cdot\text{dm}^{-2}$  (Fig. 5), current efficiency decreased from 37.7 % to 34.1 %. Current efficiency increased again up to 38 % when the current density was increased from 15 to  $30 \text{ A}\cdot\text{dm}^{-2}$ . Mn concentration (wt %) detected by AAS also increased from 90.78 % to 95.03 % (Fig. 6A) when the current density increased. When the current density in the MASB with 0.55 mM Te(VI) additive increased from 2 to  $15 \text{ A}\cdot\text{dm}^{-2}$ , current efficiency decreased from 30.9 % to 29.8 % as well. However, if  $j_c$  increased to  $30 \text{ A}/\text{dm}^2$ , current efficiency increased up to 36.2 % (Fig. 5). Irrespective of the Te(VI) additive concentration, current efficiency dependence on current density has a breakpoint at the highest  $15 \text{ A dm}^{-2}$  current density, which is related with the structural transformation of electrodeposits (see 3.4). With the increasing of current density, the total concentration of tellurium (wt %) decreased from 2.22 % to 0.35 % when the concentration of Te(VI) additive in the MASB was the highest (Fig. 6B). A similar dependence was observed at the smallest and medium concentrations of Te(VI) additive in the MASB.

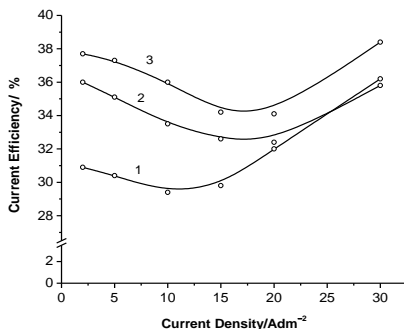


**Fig. 5.** Influence of Te(VI) additive concentration in electrolyte on current efficiency of coatings electrodeposited from MASB: **1** – 0.55 mM; **2** – 1.10 mM; **3** – 2.20 mM

Since the best quality Mn coatings were obtained in the MASB with 2.20 mM concentration of Te(VI) and at current density  $j_c = 15 \text{ A}\cdot\text{dm}^{-2}$ , further experiments were selected at the latter concentration and current density. The XPS spectra of Te 3d<sub>5/2</sub>, Mn 2p<sub>3/2</sub> and O 1s on the surface and in deeperlayers (till ~50 nm) of electrolytic Mn coatings were studied (Fig. 7). From the data gained by the XPS method, the elements' atomic percentages were calculated.

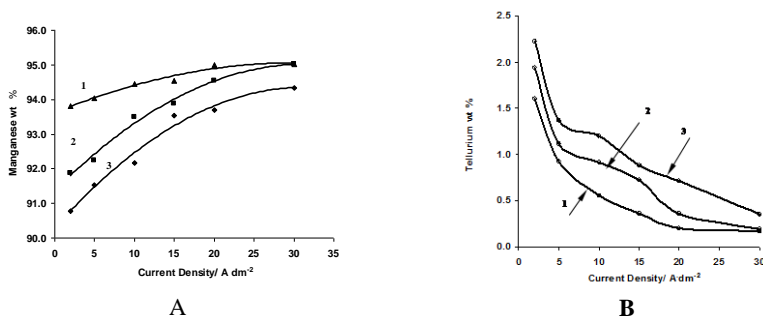


**Fig. 6.** Influence of Te(VI) additive concentration in electrolyte on concentration of manganese (A) and tellurium (B) wt % in coatings electrodeposited from MASB: **1** – 0.55 mM; **2** – 1.10 mM; **3** – 2.20 mM

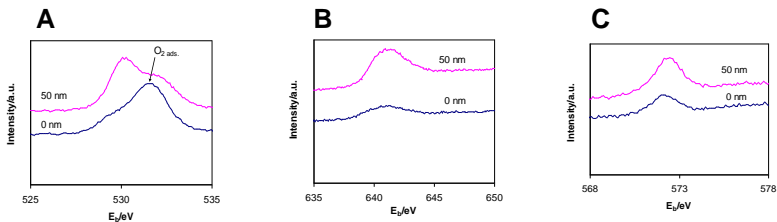


**Fig. 7.** XPS O 1s (A), Mn 2p<sub>3/2</sub> (B), Te 3d<sub>5/2</sub> (C) spectra of coatings electrodeposited from the MASB with 2.20 mM Te(VI) additive. Depth of etching is presented by the curves above

From the peak Te 3d<sub>5/2</sub>, corresponding to the binding energy ~572 eV and Mn 2p<sub>3/2</sub> peak position (640–641 eV) in XPS spectra, it is possible to assert that MnTe was formed.

A high concentration of oxygen on the coatings surface can be explained by the adsorption of air oxygen when transferring samples from the electrolytic cell to the spectrometer chamber. After etching the surface of Mn coatings up to 50 nm, the binding energy of O 1s peak differs ~2 eV. This has proven that in the deeper layers Mn is partly oxidised and consists from different oxygen compounds (MnO, Mn<sub>2</sub>O<sub>3</sub>) (Table 1).

Fig. 8 shows the GDS-derived elemental composition profiles of the coating. The samples were analyzed at successive depths until the substrate (Fe) was reached. The thickness of the manganese coatings was 15–16 μm. At the surface of the coating, a higher concentration of oxygen was present, presumably due to surface oxidation (Fig. 8A). After removing the oxide layer from the surface of the coating, the manganese concentration increased and the oxygen concentration decreased (Fig. 8B). The presence of oxygen in the deeper layers of the coating can be explained by the inclusion of Mn(OH)<sub>2</sub>/Mn<sub>x</sub>O<sub>y</sub>, produced as a result of the pH increase at the interface. When examining deeper into the coating, the Mn concentration diminished and a signal corresponding to the substrate (Fe) emerged, indicating an interface between the substrate (Fe) and deposit Mn.

**Table 1.** XPS data of Mn coatings, electrodeposited from MASB with 2.20 mM Te(VI) additive at current density 15 A·dm<sup>-2</sup>. Etching rate of coatings surface by Ar<sup>+</sup> ~5 nm min<sup>-1</sup>.

Element	Spectrum line	Etching time/min. (approx. depth/nm)	E <sub>b</sub> /eV	Cons. /atom. %	Composition
Mn	2p <sub>3/2</sub>	0 (0)	641.2	35.28	MnTe, MnO and/or Mn <sub>2</sub> O <sub>3</sub>
		10 (50)	640.8; 641.5	52.42	MnTe, Mn <sub>(met.)</sub> , MnO and/or Mn <sub>2</sub> O <sub>3</sub>
O	1s	0 (0)	531.7	64.01	O <sub>2(ads.)</sub>
		10 (50)	529.8; 530.2	45.75	MnO and/or Mn <sub>2</sub> O <sub>3</sub>
Te	3d <sub>5/2</sub>	0 (0)	571.9	0.71	MnTe
		10 (50)	572.2	1.83	MnTe

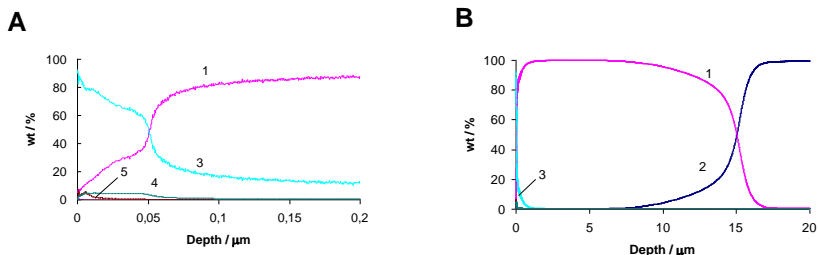


**Fig 8.** GDS elemental-distribution profiles (**A** – low depth; **B**– high depth) of a coating electrodeposited from MASB with 2.20 mM Te(VI) additive at current density 15 A·dm<sup>-2</sup>: 1– Mn, 2 – Fe, 3 – O, 4 – C, 5 – S

### 2.1.3. X-ray diffraction study and morphology

XRD analysis was used for the determination of the manganese structure. Coatings for this analysis were electrodeposited at current density 15 A·dm<sup>-2</sup>. Tellurium or manganese telluride phases were not detected in coatings electrodeposited from the MASB with the smallest and highest concentrations of Te(VI) additive. It is associated with the relative low concentration of

incorporated tellurium in the coatings. XRD analysis has shown that the coatings electrodeposited at the lowest and medium current densities ( $j_c = 2\text{--}15 \text{ A}\cdot\text{dm}^{-2}$ ) consist of a mixture of two modifications: brittle  $\alpha$ -Mn (body-centeredcubic) and plastic  $\beta$ -Mn (cubic). A stronger structural change was observed in the Mn coatings, electrodeposited at the highest current densities: in coating, electrodeposited at  $20 \text{ A}\cdot\text{dm}^{-2}$ , modification of  $\alpha$ -Mn predominated and in electrodeposit, obtained at  $30 \text{ A}\cdot\text{dm}^{-2}$ , the clear crystalline structure disappeared, coating became amorphous (Fig. 9).

SEM analysis has shown that Mn coatings have fine grain morphology. Coatings obtained at  $15 \text{ A}\cdot\text{dm}^{-2}$  from the MASB with  $0.55\text{--}2.20 \text{ mM}$  of Te(VI) additive have an uncertain form of crystallites (Fig. 10). EDX analysis of the coatings surface performed together with SEM analysis has shown that irrespective of Te(VI) additive concentration in the MASB, the bottom-parts of morphology (in comparison with the top-parts) have a higher concentration (atom. %) of tellurium. This difference decreases with the increasing of Te(VI) additive concentration in the MASB (Table 2). This confirms an assumption that most of the tellurium incorporates in electrodeposits at the initial stage of electrolysis.

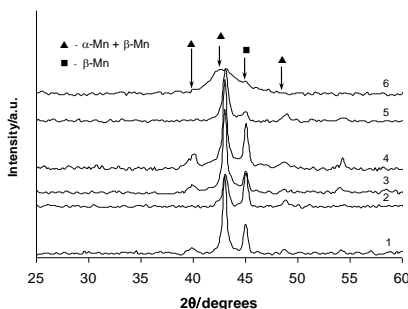


**Fig. 9.** X-ray diffraction patterns of coatings electrodeposited from MASB with  $2.20 \text{ mM}$  Te(VI) additive at different current densities : **1**–  $2 \text{ A}\cdot\text{dm}^{-2}$ ; **2**–  $5 \text{ A}\cdot\text{dm}^{-2}$ , **3**–  $10 \text{ A}\cdot\text{dm}^{-2}$ ; **4**–  $15 \text{ A}\cdot\text{dm}^{-2}$ ; **5**–  $20 \text{ A}\cdot\text{dm}^{-2}$ ; **6**–  $30 \text{ A}\cdot\text{dm}^{-2}$

The change of morphology of electrodeposits, obtained from the MASB with the highest concentration of Te(VI) additive at different current densities, is presented in Fig. 10C and Fig. 11. In the SEM images of coatings, electrodeposited at current density  $2 \text{ A}\cdot\text{dm}^{-2}$  unformed crystallites are still observed, whereas at  $20 \text{ A}\cdot\text{dm}^{-2}$  small crystallites show up. Transformation of crystalline structure of coatings (they become more compact) with increasing current density causes cracking of the Mn coating (especially at  $20 \text{ A}\cdot\text{dm}^{-2}$ ).



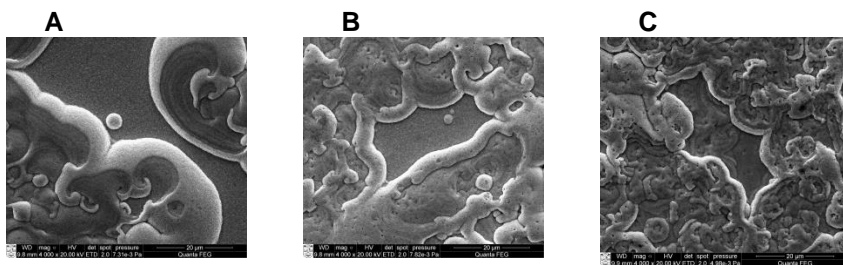


**Fig. 10.** SEM images of electrodeposits obtained from MASB with different concentrations of Te(VI) additive at current density  $15 \text{ A}\cdot\text{dm}^{-2}$ : **A** – 0.55 mM; **B** – 1.10 mM; **C** – 2.20 mM. Magnitude  $\times 4000$

**Table 2.** Distribution of Te (atom. %) in coatings electrodeposited from MASB with different concentrations of Te(VI) additive at current density  $15 \text{ A}\cdot\text{dm}^{-2}$

	Analyzed places of coating surface	Concentration of Te(VI) additive in MASB/mM		
		0.55	1.10	2.20
Te atom. %	Bottom-part	1.08	0.97	0.61
	Top-part	0.41	0.42	0.55

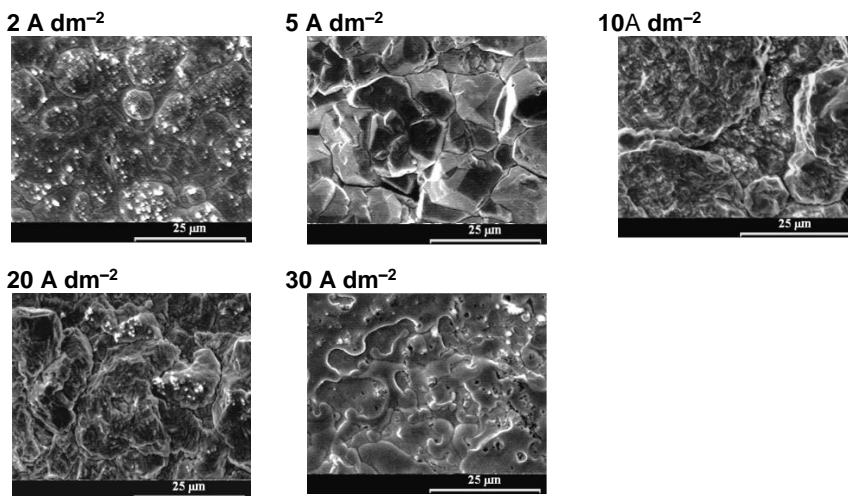


**Fig. 11.** SEM images of Mn electrodeposits obtained from MASB at different current densities. Concentration of Te(VI) additive 2.20 mM. Magnitude  $\times 2000$

#### 2.1.4. Mechanical properties

Dependence of internal stresses on current density was studied. Tensile stresses are characteristic of electrolytic Mn coatings, which have been

electrodeposited from electrolytes without additives. Our experimental data suggests that changing of current densities in the MASB with Te(VI) additive influences large tensile stresses of deposited coatings as well. It was determined, that the maximal tensile stress values were obtained at the initial stage of electrolysis, namely when passing relatively small amounts of electric charge (160–180 As through 1000 mm<sup>2</sup> surface area). We presume that this is related to the primary Mn layer formation with a higher concentration of incorporated Te around the Fe cathode surface. After full coating, the electrodeposited on the cathode surface, the tension stresses varied little. The smallest tension stresses were measured for the Mn coatings electrodeposited at current density 2 A·dm<sup>-2</sup>, and the largest ones were determined when current density was 15 A·dm<sup>-2</sup> (Fig.12). We presume that this is likely associated with the changes in structure (see 3, 4).

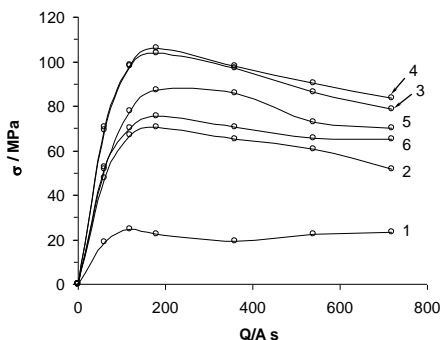


**Fig. 12.** Influence of current charge  $Q$  on tension stresses of Mn obtained from MASB with 2.20 mM Te(VI) additive at different current densities (A dm<sup>-2</sup>): 1 – 2; 2 – 5; 3 – 10; 4 – 15; 5 – 20; 6 – 30

As mentioned above, Te incorporates in Mn coatings and change their structure and morphology. That also influences microhardness of the coatings. Usually, an increase in Mn concentration in coatings also increases their microhardness. In this case, it was determined that Mn concentration (wt %) was slightly different: 90.7 and 93.3 % (at 2 A dm<sup>-2</sup> and at 15 A dm<sup>-2</sup>, respectively). Therefore, a decrease in microhardness from HV = 2721.6±32.6 Pa to HV = 1820.2±11.96 Pa (at 2 A dm<sup>-2</sup> and at 15 A dm<sup>-2</sup>, respectively) was associated with the variation of the total Te concentration in electrodeposits. The highest concentration (wt %) of incorporated Te in Mn coatings was obtained at 2 A·dm<sup>-2</sup> and reached 2.22 %, and it was only 0.88 % at 15 A·dm<sup>-2</sup>.

## 2.2. Influence of temperature on Mn electrodeposition

### 2.2.1. Composition and current efficiency

The compositional analysis performed by AAS has shown that with the increase of temperature of the MASB with Te(VI) additive from 20 to 80 °C, the total concentration of Mn in the obtained coatings decreased slightly from 99.1 to 98.4 wt. % (Fig. 14). Meanwhile, the concentration of Te in the obtained coatings increased from 0.9 to 1.6 wt. % (Fig. 13). The incorporation mechanism of Te into Mn coatings and the influence of Te or its compounds on the electrodeposition process of Mn were discussed thoroughly enough in several papers.

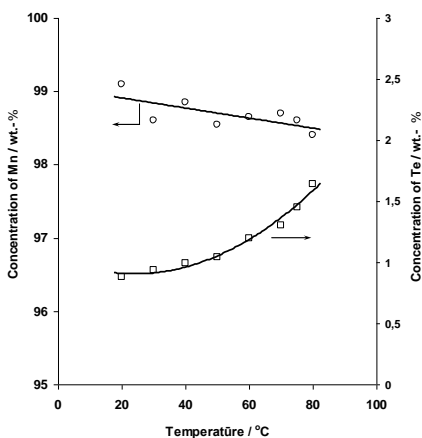


**Fig. 13.** Influence of temperature on Mn and Te concentrations (wt.-%) in Mn coatings obtained from MASB with 2.20 mM Te(VI) additive at  $j_c = 15 \text{ A}\cdot\text{dm}^{-2}$

It was observed that the current efficiency of the coatings electrodeposited at the  $j_c=15 \text{ A}\cdot\text{dm}^{-2}$  showed a weak exponential dependence on the temperature and its values increased almost twice (from 37 % to 71 %) when the temperature of the MASB increased from 20 to 80 °C (Fig. 14).

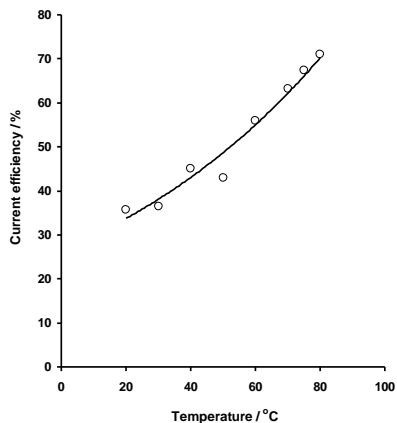


**Fig. 14.** Influence of temperature on current efficiency of Mn coatings obtained from MASB with 2.20 mM of Te(VI) additive at  $j_c = 15 \text{ A}\cdot\text{dm}^{-2}$

This observation can be partially explained by the increase of the pH value of the MASB with the increase of temperature. The concentration of hydrogen ions in the MASB decreased exponentially by ca. 4 times when the temperature of the MASB increased from 20 to 80 °C. It is known that during electrodeposition, the pH value near the cathode layer can increase up to one unit (i.e. concentration of  $\text{H}^+_{(\text{aq})}$  ions decreases by ca. 10 times) in the MASB at room temperature. Ultimately, this leads to the significant drop of partial discharging current of  $\text{H}^+_{(\text{aq})}$  ions and to the decrease of the evolution rate of gaseous hydrogen on the Mn electrodeposit. On the other hand, the increased concentration of Te incorporated into Mn coatings, observed at the higher temperatures, could additionally reduce the self-dissolving (corrosion) rate of Mn in an acidic MASB.

The surface analysis of the Mn coatings performed by EDX in the “point mode” (together with SEM analysis) showed that the surface concentration of Te differs on the lower and on the upper parts of the morphology (on the pits and on the bumps, respectively). Such a difference was also observed in our previous paper. The greatest differences of the Te concentration in upper and lower parts of morphology were observed for coatings obtained from the MASB at the lower temperatures (Fig. 15). The difference of the Te concentrations decreases with the increase of temperature of the MASB. This observation can apparently be explained by the formation of smoother Mn coatings at the elevated temperatures. This assumption was confirmed by the measurements of roughness performed with AFM. The difference in the Te concentrations determined by the different techniques (AAS and EDX) is related to the morphological artefacts of intrinsically local quantitative EDX analysis, especially for alloys.

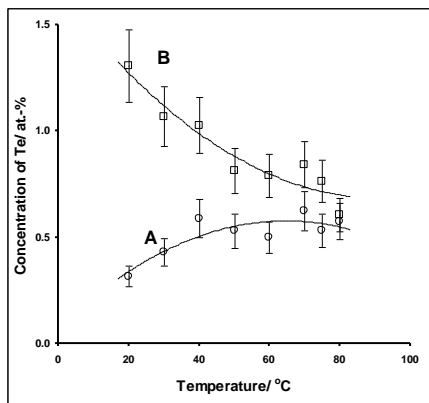


**Fig. 15.** Influence of temperature on distribution of Te in upper (curve A) and lower (curve B) parts of Mn coatings obtained from MASB with 2.20 mM of Te(VI) additive at  $j_c = 15 \text{ A}\cdot\text{dm}^{-2}$

### 2.2.2. X-ray diffraction study and morphology

As mentioned above, Te incorporates into Mn coatings and changes their structure and morphology. The XRD analysis showed that the coating obtained at  $j_c = 15 \text{ A}\cdot\text{dm}^{-2}$  at a room temperature (20 °C) consists of the mixture of two phase modifications: hard and brittle  $\alpha$ -Mn (body-centered cubic) phase and plastic  $\beta$ -Mn (cubic) phase. Smooth changes in the structure were observed for Mn coatings obtained from the MASB with Te(VI) additive at increased temperatures (30–50 °C). When the temperature of the MASB was higher than 50 °C, the structure of Mn coatings changed considerably (Fig. 16):  $\beta$ -Mn phase (characteristic peaks at  $2\Theta \sim 45^\circ$  and  $\sim 69^\circ$ ) disappeared and the harder  $\alpha$ -Mn phase remained. Such a change was also observed by other authors when electroplating at 60 °C produced deposits composed completely of the  $\alpha$ -Mn phase.

The calculation of the average size of the crystallites showed that the coatings obtained from the MASB with Te(VI) additive at  $j_c = 15 \text{ A}\cdot\text{dm}^{-2}$  and in full range of the chosen temperatures are nanocrystalline (Fig. 17). The variation of the full width at half maximum of the peaks of  $\alpha$ -Mn and  $\beta$ -Mn phases indicated that the size of crystallites decreased with the increase of temperature of the MASB. The size of crystallites of Mn coatings obtained at 20 °C was found to be ca. 25 nm, whereas the size of crystallites reached only approx. 12 nm at the highest temperature (80 °C) (Fig. 17). A similar decrease of the surface roughness values of Mn coatings with the increase of the MASB temperature was observed by AFM (Table 3).

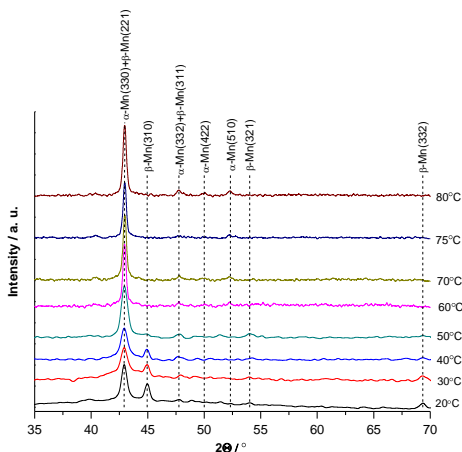


**Fig. 16.** X-ray diffraction patterns of Mn coatings obtained from MASB with 2.20 mM of Te(VI) additive at  $j_c = 15 \text{ A}\cdot\text{dm}^{-2}$  and different temperatures

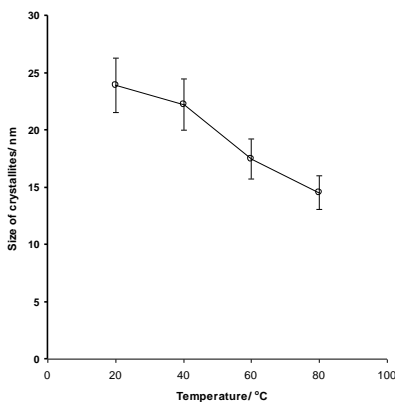


**Fig. 17.** Influence of temperature on mean crystallites sizes of Mn coatings obtained from MASB with 2.20 mM Te(VI) additive at  $j_c = 15 \text{ A}\cdot\text{dm}^{-2}$ . Calculation performed from characteristic peaks at  $2\theta \sim 43^\circ$  and  $\sim 45^\circ$

Figure 18 illustrates the changes of morphology of Mn coatings, obtained from the MASB with the additive of Te(VI) at  $j_c = 15 \text{ A}\cdot\text{dm}^{-2}$  observed at the different temperatures. The SEM images showed the uncertain form of fine grains on the surface of Mn deposits obtained at 20–40 °C. When the temperature of the MASB was 50 °C and higher, the cube-shaped grains of various dimensions appeared on the surface of the obtained Mn coatings.

**Table 3.** Roughness, average height and skewness values detected by AFM for Mn coatings, obtained from MASB with 2.20 mM Te(VI) additive at  $j_c = 15 \text{ A}\cdot\text{dm}^{-2}$  and different temperature

Dimension	Temperature, °C			
	20	40	60	80
Root mean square roughness $R_q$ , nm	178.57	130.28	76.48	30.39
Average roughness $R_a$ , nm	145.10	101.20	60.12	23.05
Average height $Z_{\text{mean}}$ , nm	682.15	562.23	269.33	115.15
Skewness, $R_{sk}$	-0.15	-0.20	0.03	0.48

### 2.2.3. Mechanical properties

The previous study showed that the increasing of the cathodic current densities from 2 to 15  $\text{A}\cdot\text{dm}^{-2}$  lead to the exhibition of large tensile stresses in Mn coatings obtained from the MASB with Te(VI) additive at room temperature. In the present study, the tensile stresses were estimated only for Mn coatings obtained in the temperature range from 20 to 60 °C. The experimental data of tensile stresses at a temperature of 70 °C and higher could not be accessed because of technical limitations (increased evaporation of water from electrolyte leads to an adverse event, i.e. water steam condensation on the optical parts of microscope of the measuring equipment, which hinder the measurement). Figure 19 shows that with the increasing of temperature of the electrolyte, the maximum tensile stress values of the obtained Mn coatings decreased from 106 MPa to 76 MPa (measured at 20 and 60°C, respectively). In the whole temperature range chosen, as well as at 20 °C, the maximum tensile stress values of the obtained Mn electrodeposits were observed at the initial period of the formation, i. e. when the thickness of the Mn coatings were 1.5–2.0  $\mu\text{m}$ . The slight relaxation of tensile stresses was observed with the increase of the thickness of electrodeposits.

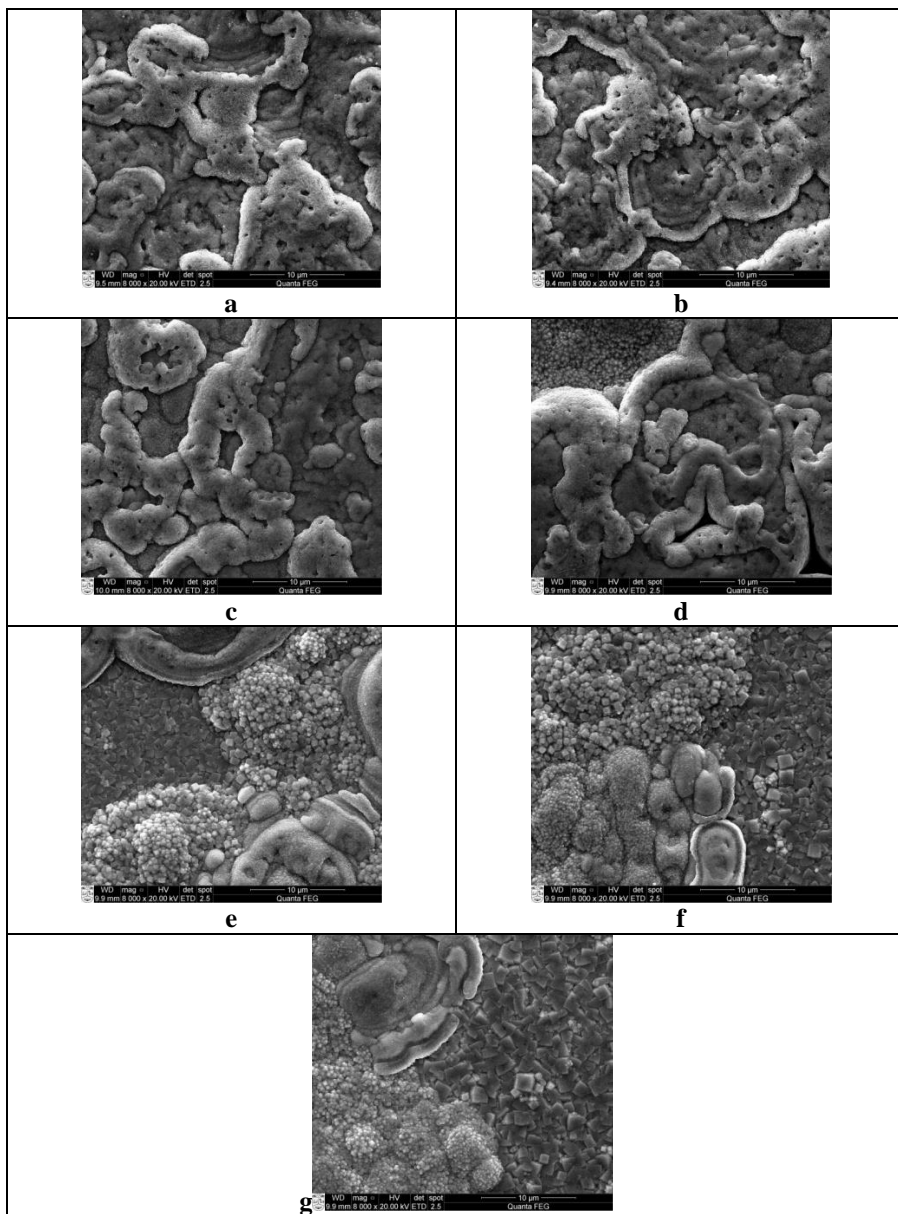


**Fig. 18.** SEM images of Mn coatings obtained from MASB with 2.20 mM of Te(VI) additive at  $j_c = 15 \text{ A} \cdot \text{dm}^{-2}$  and different temperature: **a** 20 °C; **b** 30 °C; **c** 40 °C; **d** 50 °C; **e** 60 °C; **f** 70 °C; **g** 80 °C. Magnitude x8000



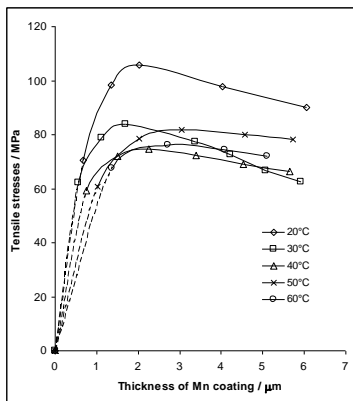


**Fig. 19.** Dependence of tensile stresses on thickness of Mn coatings obtained from MASB with 2.20 mM of Te(VI) additive at  $j_c = 15 \text{ A}\cdot\text{dm}^{-2}$  and different temperature

Microhardness, by Vickers, of Mn coatings obtained from the MASB with Te(VI) additive at  $a_{j_c} = 15 \text{ A}\cdot\text{dm}^{-2}$  was tested in the full range of temperatures. An increase of temperature from 20 to 50 °C of the MASB lead to the decrease of microhardness of Mn coatings from 1820 MPa to 1452 MPa. It is apparently related with the structural changes of the coatings containing the mixture of  $\alpha$ -Mn and  $\beta$ -Mn phases. The values of microhardness of Mn coatings obtained at higher temperatures increased considerably from 1984 MPa (at 20 °C) to 2772 MPa and 3700 MPa (at 70 °C and 80 °C, respectively). This observation can apparently be explained by the increase of the total concentration of Te in the Mn electrodeposits and by predomination of the hardened  $\alpha$ -Mn phase in them.

### 3. Corrosion properties of Mn coatings

At the initial moment of immersion into a 3% NaCl solution, the corrosion potentials of Mn coatings deposited from the MASB with 2.20 mmol/l Te (VI) additive at cathode current density  $15 \text{ A}/\text{dm}^2$  and at 20 °C to 80°C, are very similar and fall into the -1250 – -1300 mV range. During the first day, corrosion potential of Mn coatings deposited from a 20°C MASB increased the most, namely up to -1100 mV, the coating deposited at 40 °C increased very slightly, i.e. up to -1200 mV, while the potential for the coatings deposited from 60 °C and 80 °C in the MASB remained almost unchanged (Fig.20 a). During the 2-4 days, potentials of Mn coatings deposited at 20 °C, 40 °C and 60 °C gradually increased to -1070 mV, -1140mV and -1190 mV, respectively. During the 5-10 days, potentials of Mn coatings deposited from 20 °C and 40 °C in the MASB remained stable, whereas the results for the coatings deposited at 60 °C

continued to increase. Meanwhile, within 2-10 days, potential of the Mn coatings deposited at 80 °C increased very slightly up to -1250 mV, but its value remained the lowest (Fig.20 b).

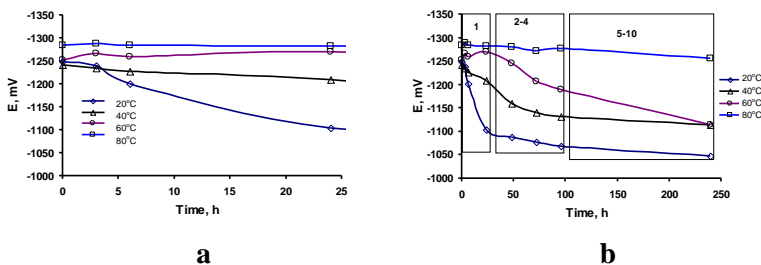


**Fig. 20.** Change in potential value for the Mn coatings obtained from MASB with 2.2mM Te(VI) additive at current density  $j_c = 15 \text{ A}\cdot\text{dm}^{-2}$  over time: a – in 1 day, b – in 1-10 days

The calculated corrosion current strengths of Mn coatings, which are directly proportional to the corrosion rate of these coatings and their function of time (Fig. 21), showed that Mn coatings electrodeposited from the MASB with 2.20 mM Te (VI) additive at 20°C and 40°C and cathode current density  $15 \text{ A}\cdot\text{dm}^{-2}$  corroded the fastest at the initial moment of the immersion into a corrosive medium, but after 1 day corrosion slowed down from 4 to 2 times, whereas after 3-10 days these coatings corroded 2.5-3 times slower than at the moment of initial immersion into the corrosive medium. This can be explained by the formation of a corrosion product film, which possesses good protective properties and provides passivation of the coatings surface. Meanwhile, the coatings electrodeposited from the MASB with 2.20 mM Te (VI) additive at 60°C and cathode current density  $15 \text{ A}\cdot\text{dm}^{-2}$  corroded the slowest at the initial immersion moment, but after 1 day their corrosion intensified because  $I_{corr}$  increased nearly 2 times. After 3-10 days,  $I_{corr}$  of these Mn coatings suddenly decreased, almost to the original level and the corrosion rate was close to that of the Mn coatings deposited from the MASB at 20°C and 40°C. The constant decreasing of  $I_{corr}$  values and thus the corrosion rate over time is characteristic of the Mn coatings deposited from the MASB at 80°C. Corrosion of such coatings intensified almost twice within 1-3 days, and after 10 days the corrosion current strength was 4 times higher than the one at the initial moment. It could be associated with the corrosive activity of the Mn coating itself, due to the possible surface defects and formation of the poorly adhering, fluffy film of corrosion products on the surface of these coatings.

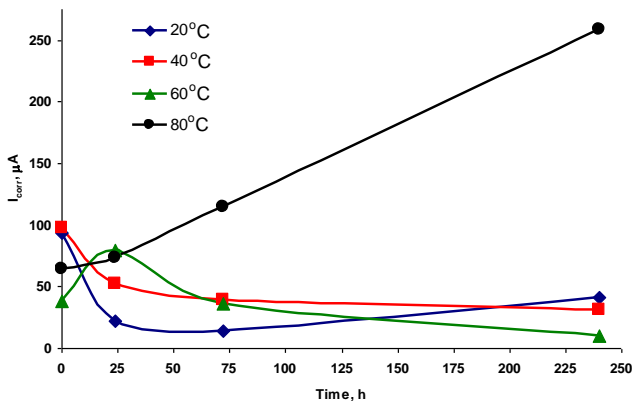


**Fig. 21.** Change in corrosion current strength  $I_{corr}$  for Mn coatings deposited from the MASB with 2.20 mM Te (VI) additive at current density  $j_c = 15 \text{ A}\cdot\text{dm}^{-2}$  in naturally aerated 3 % aqueous NaCl solution over time

Semi-logarithmic corrosion potentiodynamic polarization curves recorded in 3 % aqueous NaCl solution at the initial moment of immersion into a corrosive medium for the Mn coatings deposited from the MASB with 2.20 mM Te (VI) additive at 20 °C and cathode current density 10-20  $\text{A}\cdot\text{dm}^{-2}$  (Fig. 22), "Tafel approximation" of these curves, and calculation of corrosion equilibrium potential  $E_{corr}$  and corrosion current strength  $I_{corr}$  values of these coatings (Table 4) have revealed that the Mn coatings deposited at cathode current density 10  $\text{A}\cdot\text{dm}^{-2}$  and 15  $\text{A}\cdot\text{dm}^{-2}$  have the highest (most electropositive) and closest to each other (differing only by 6 mV) values of corrosion equilibrium potential. Whereas, the value of corrosion equilibrium potential of Mn coating deposited at cathode current density 20  $\text{A}\cdot\text{dm}^{-2}$  is significantly lower (more electronegative). The values of the corrosion current strength  $I_{corr}$  for the Mn coatings deposited at cathode current density 10  $\text{A}\cdot\text{dm}^{-2}$  and 15  $\text{A}\cdot\text{dm}^{-2}$  are also very close and more than four times lower than that for the Mn coating deposited at cathode current density 20  $\text{A}\cdot\text{dm}^{-2}$ .

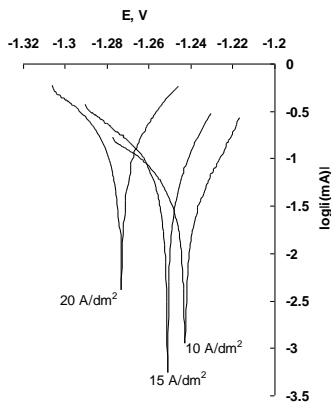
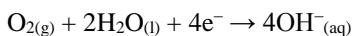


**Fig. 22.** Corrosion potentiodynamic polarization curves of the Mn coatings deposited from the MASB with 2.20 mM Te (VI) additive at 20 °C and different cathodic current density in naturally aerated 3% aqueous NaCl solution at the initial moment of immersion into corrosive medium

**Table 4.** Kinetic parameters of the Mn coatings deposited from the MASB with 2.20 mM Te (VI) additive at 20 °C and different cathodic current density in naturally aerated 3% aqueous NaCl solution at the initial moment of immersion into corrosive medium

MASB temperature, °C	$i_k$ , A/dm <sup>2</sup>	$E_{cor}$ , mV	$I_{cor}$ , μA	$\beta_c$ , mV/decade	$\beta_a$ , mV/decade
20	10	-1245	83.4	89.8	77.3
	15	-1251	93.6	66.7	37.5
	20	-1271	408.2	135.7	104.8

Therefore, in all the cases examined, the Tafel constant value of cathodic corrosion process is greater than the one of the anodic corrosion process ( $\beta_c > \beta_a$ ), based on the literature data, it may be assumed that Mn corrosion is limited by the cathode process, i. e. oxygen depolarization resulting in formation of hydroxide ions:



Anodic corrosion process is oxidation of manganese:



In order to better identify the behavior of electrolytic Mn coatings in protecting steel base against corrosion over a longer period of time, they have

been tested in a salt spray atmosphere. Corrosion resistance of manganese coatings was evaluated gravimetrically according to the change in mass per area unit over time. The tests in a chamber of the salt spray showed that sample mass increased over time due to the formation of slightly soluble and insoluble corrosion products on the surface of the coatings (Fig.23). An accurate calculation of the corrosion rate according to the mass increase per area unit ( $\Delta m/S$ ) requires the identification of corrosion products and their quantitative composition. The measurement results of coating mass increase are influenced by the dissolution of corrosion products themselves and their adhesion to the Mn coating. The experiment becomes very complicated and inaccurate, therefore the increase in mass of the sample can provide just preliminary information about the corrosion activity of electrolytic Mn coatings.

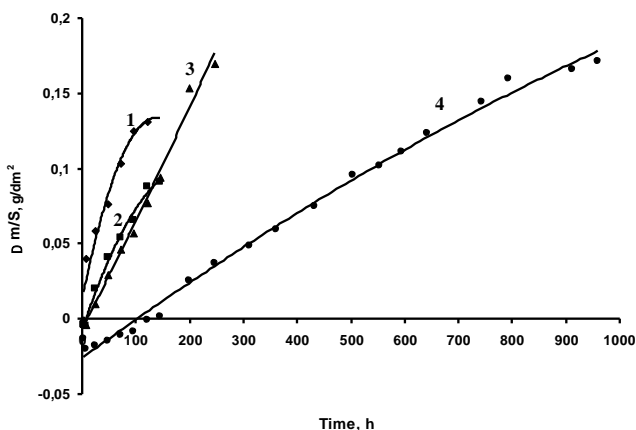


**Fig. 23.** Dependence of mass increase per area unit for the Mn coatings deposited from MASB at 20 ° C on the duration of presence in salt spray chamber: 1-5 A·dm<sup>-2</sup>; 2-10 A·dm<sup>-2</sup>; 3-15 A·dm<sup>-2</sup>; 4-15 A·dm<sup>-2</sup> + FD

As seen from Figure 23, the corrosion products are formed quicker and in larger quantity on the surface of the Mn coatings deposited from the MASB at  $j_c = 5-10 \text{ A}\cdot\text{dm}^{-2}$ . These samples were removed from the salt spray chamber after  $\sim 144 \text{ h}$ , when Mn coatings were fully corroded and the steel substrate was visible. The corrosion of Mn coatings deposited at  $15 \text{ A}\cdot\text{dm}^{-2}$  corroded in 246 h (Fig. 23 curve 3). The mass of Mn coating coated with Phosphate coating initially decreased as the soluble phosphatic film (23, Fig. 4 curve) was dissolving first.

The change in color over time resulting from the corrosion products formed on the surface of the Mn coatings can be evaluated visually, after removing the

coating from the salt spray chamber. For the longest period of time (even 546 h) corrosion products did not form on the surface of Mn coatings coated with phosphate coating. When the MASB temperature was increased, fewer corrosion products formed (Fig. 24). The most corrosion resistant towards Mn coatings were the ones deposited at 80 °C; they only corroded after 546 h.

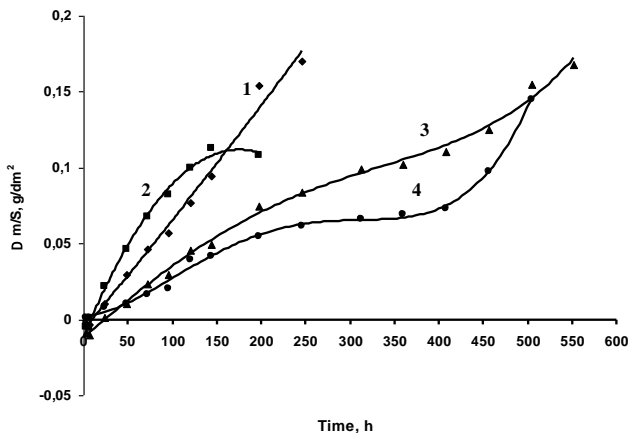


**Fig. 24.** Dependence of mass increase per area unit for the Mn coatings deposited from MASB at 15 A·dm<sup>-2</sup> current density on the duration of presence in salt spray chamber: 1 – 20°C; 2 – 40°C; 3 – 60°C; 4 – 80°C.

The data of XRD analysis has revealed that during corrosion of the Mn coatings in the fog of a neutral NaCl solution, dense brown corrosion products, predominantly MnO<sub>2</sub>, Mn<sub>3</sub>O<sub>4</sub> and MnCO<sub>3</sub>, which slow down the further corrosion are formed on the surface of Mn.

The change in color over time resulting from the corrosion products formed on the surface of the Mn coatings deposited from the MASB at different temperatures can be evaluated visually, after removing the coating from the salt spray chamber. It has been determined that resistance of the coatings against corrosion increases with the increasing deposition temperature.

The salt spray chamber tests have shown that Mn coatings, coated with phosphate coating, protect the steel base against corrosion much longer in comparison with not phosphatized Mn coatings. Corrosion products formed much later on the phosphatized Mn coating (Fig. 23). In the case of phosphatized Mn coatings, when the samples were removed from the salt spray chamber after 546 hours, not the entire coating surface was corroded. Straw-shaped crystallites of phosphate coating were seen on the surface of the remaining Mn coating, thus proving that phosphatic coating increases the corrosion resistance of the Mn coating.

## CONCLUSIONS

1. Electrolytic Mn coatings are electrodeposited from the stable manganese ammonium sulphate bath (0.95 mol/l  $(\text{NH}_4)_2\text{SO}_4$ , 0.62 mol/l  $\text{MnSO}_4 \cdot 5\text{H}_2\text{O}$ , pH = 2.3, with Te (VI) additive, which is obtained from sodium telluratum  $\text{Na}_2\text{TeO}_4 \cdot 2\text{H}_2\text{O}$ ).

2. Elemental Te, formed on the cathode surface, depolarizes the cathodic process and determines further origination of the limit current of the higher value at the -1.1 – -1.3 V potential range. It has been determined that at this potential range, separate MnTe crystallites are formed on the surface of the carbon steel cathode.

3. Tellurium incorporated into electrodeposited Mn coatings at the initial stage of electrolysis affects the structure and morphology of the coatings. Electrolytic Mn coatings deposited at  $j_c = 2\text{--}10 \text{ A} \cdot \text{dm}^{-2}$  consist of the mixture of two phase modifications: hard and brittle  $\alpha$ -Mn phase and plastic  $\beta$ -Mn phase. More significant structural changes have been detected for the Mn coatings electrodeposited at higher current densities.

4. With an increasing electrolyte temperature from 20 °C to 80 °C, the structure of the coating changes: mixture of the  $\alpha$ -Mn and  $\beta$ -Mn modifications is replaced by  $\alpha$ -Mn one. The current efficiency of electrolytic Mn coating increases from 37 to 71 % ( $j_c = 15 \text{ A} \cdot \text{dm}^{-2}$ ) and Te concentration increases from 0.9 to 1.6 %.

5. Electrolytic Mn coatings, electrodeposited from the MASB with 2.2 mmol/l Te(VI) additive at current density 2 – 30  $\text{A} \cdot \text{dm}^{-2}$ , are nanocrystalline. The average size of the crystallites decreases from 75 nm to 18–26 nm with the increasing current density. The increase of electrolyte temperature from 20 to 80 °C decreases the average size of the crystallites from 25 to 15 nm ( $j_c = 15 \text{ A} \cdot \text{dm}^{-2}$ ).

6. Irrespective of the concentration of Te(VI) additive in the MASB, the concentration of tellurium is higher in the pits of the Mn coatings in comparison with the one in the bumps. However, this difference decreases with the increasing concentration of Te(VI) additive in the MASB. The greatest difference in these concentrations has been determined for the coatings electrodeposited at 20 °C. This difference decreases when the temperature of the MASB increases from 20 to 80 °C

7. Electrolytic Mn coatings electrodeposited at 20 °C exhibit large tensile stresses. The lowest tensile stresses ( $\sigma \sim 22 \text{ MPa}$ ) have been determined at  $j_c = 2 \text{ A} \cdot \text{dm}^{-2}$ , the largest ones ( $\sigma \sim 91 \text{ MPa}$ ) were recorded at  $j_c = 10\text{--}15 \text{ A} \cdot \text{dm}^{-2}$ .

8. Te incorporated into Mn coatings influences microhardness of the coatings. An increase in current density leads to the decrease of Mn coating microhardness from  $2721.6 \pm 32.6$  to  $1820.2 \pm 11.96 \text{ MPa}$ . Whereas, the increase of electrolyte temperature decreases microhardness of the highest quality Mn

coatings from  $1820.2 \pm 11.96$  to  $1452.3 \pm 17.4$  Mpa. At a temperature higher than  $60\text{ }^\circ\text{C}$ , it increases to  $2772.2 \pm 58.4$  MPa.

9. Corrosion kinetic parameters for Mn coatings and data of the experiments in the salt spray chamber have indicated the Mn coatings, containing Te, electrodeposited at  $15\text{ A}\cdot\text{dm}^{-2}$  current density are the most resistant towards corrosion. The resistance of the coatings increases significantly after coating them with phosphate film.

### **List of Publications and proceedings on the Theme of the Dissertation Publications corresponding to the list of the Institute of Science Information (ISI) database**

1. Galvanauskaitė, Nerita; Šulčius, Algirdas; Griškonis, Egidijus; Diaz-Arista, P. Influence of Te(VI) additive on manganese electrodeposition at room temperature and coating properties // Transactions of the Institute of Metal Finishing. Leeds : Maney Publishing. ISSN 0020-2967. 2011, Vol. 89, no. 6, p. 325-332.

2. Šulčius, Algirdas; Griškonis, Egidijus; Kantminienė, Kristina; Žmuidzinavičienė, Nerita. Influence of different electrolysis parameters on electrodeposition of  $\gamma$ - and  $\alpha$ -Mn from pure electrolytes — a review with special reference to Russian language literature // Hydrometallurgy. Amsterdam : Elsevier Science. ISSN 0304-386X. 2013, vol. 137, p. 33-37.

3. Griškonis, Egidijus; Šulčius, Algirdas; Žmuidzinavičienė, Nerita. Influence of temperature on the properties of Mn coatings electrodeposited from the electrolyte containing Te(VI) additive // Journal of applied electrochemistry. Dordrecht : Springer. ISSN 0021-891X. 2014, Vol. 44, is. 10, p. 1117-1125.

P.S. In 2012, The Institute of Materials Finishing (IMF, Birmingham, United Kingdom) has awarded the authors of the manuscript “Influence of Te(VI) additive on manganese electrodeposition at room temperature and coating properties” the Westinghouse Prize (Sponsored by Riley Industries Ltd) for the best paper published in the journal “Transactions of Institute of Metal Finishing” (Trans IMF), that has shown the most valuable development in the science and practice of electrochemistry in general and electrodeposition in particular.

### **Articles in Lithuanian Journals Approved by the Department of Science and Studies**

1. Galvanauskaitė, Nerita; Griškonis, Egidijus; Šulčius, Algirdas. Mn-Te elektrolitinis nusodinimas: elektrolito paieška ir poliarizacijos tyrimai // Cheminė technologija / Kauno technologijos universitetas. Kaunas : Technologija. ISSN 1392-1231. 2010, nr. 2(55), p. 13-17.

2. Šulčius, Algirdas; Žmuidzinavičienė, Nerita; Griškonis, Egidijus; Jezerskaitė, Angelė. Mn elektrolitinių dangų, nusodintų iš sulfatinio elektrolito



su Te(VI) priedu esant skirtingoms temperatūroms, mechaninės savybės // Cheminė technologija / Kauno technologijos universitetas. Kaunas : KTU. ISSN 1392-1231. 2012, nr. 4(62), p. 10-15.

### Publications in Proceedings of Conferences

1. Galvanauskaitė, Nerita; Griškonis, Egidijus; Šulčius, Algirdas. Elektrolitinių Mn-Te lydinio dangų kietumas // Neorganinių junginių chemija ir technologija = Chemistry and technology of inorganic compounds : konferencijos pranešimų medžiaga / Kauno technologijos universitetas. Kaunas : Technologija, 2010, ISBN 9789955258025. p. 44-45.

2. Griškonis, Egidijus; Galvanauskaitė, Nerita; Šulčius, Algirdas. Selenato ir telūrato priedų įtaka mangano dangų korozijos potencialui // Neorganinių medžiagų chemija ir technologija = Chemistry and technology of inorganic materials : konferencijos pranešimų medžiaga / Kauno technologijos universitetas. Kaunas : Technologija, 2011, ISBN 9789955259817. p. 46.

3. Žmuidzinavičienė, Nerita; Šulčius, Algirdas; Griškonis, Egidijus. Electrodeposition of nanocrystalline Mn coatings // Chemistry and chemical technology 2015 : programme and proceedings of the international conference, Vilnius, Lithuania, January 23, 2015 / Vilnius University, Lithuanian Academy of Sciences, Kaunas University of Technology, Center for Physical Sciences and Technology. [S.l. : s.n., 2015], ISBN 9786094594618. p. 170-171.

### CURRICULUM VITAE

Surname, name: Žmuidzinavičienė, Nerita  
Nationality: Lithuanian  
E-mail: nerita.galvanauskaite@ktu.lt  
Education: 1991–1996 Vilnius University of Educational Sciences, Faculty of Sciences and Technology: BSc  
2006–2008 Kaunas University of Technology, Faculty of Chemical Technology: MSc in Chemical Engineering  
2010–2015 Doctoral degree studies at Kaunas University of Technology, Faculty of Chemical Technology

Area of scientific Interests: Photocatalysis, Physical chemistry, Electrodeposition

### REZIUMĖ

**Temos aktualumas.** Pastaruoju metu katodinei plieno apsaugai nuo korozijos naudojamos įvairių metalų dangos. Manganui, koroduojančiam neutralioje ar bazinėje terpėje, būdinga savo paviršiuje sudaryti netirpių

korozijos produktų plėvelę, kuri mažina tolesnę mangano koroziją. Elektrolitinio mangano dangos puikiai tinka katodinei plieno apsaugai nuo korozijos. Kai kuriose terpėse ir net tada, kai danga yra akyta arba nevientisa, manganas geriau nei cinkas saugo plieną nuo korozijos.

Mn dangų elektrolitinio nusodinimo procesą teigiamai veikia neorganiniai S, Se ir Te junginiai, ištirpinti kaip priedai, amoniakiniame sulfatiniame manganavimo elektrolite. Literatūroje nėra daug duomenų apie metalų elektrolitinių dangų mikrokietumo ir vidinių įtempių įtaką šių dangų korozinėms savybėms. Paminėtina tai, kad manganui, nusodintam iš amoniakinio sulfatinio manganavimo elektrolito be priedų, būdingi tempimo įtempiai. Literatūroje pateikiami fragmentiški Mn, nusodinto iš įvairios sudėties manganavimo elektrolitų su S ir Se priedais, mikrokietumo duomenys ir kai kurių metalų jonų ( $Zn^{2+}$ ,  $Cd^{2+}$  ir  $Cu^{2+}$ ) priemaišų įtaka elektrolitinių Mn dangų mikrokietumui. Žinoma, kad metalų ir jų lydinių dangų kokybę bei jų adheziją su pagrindu lemia elektrolitinių dangų vidiniai įtempiai. Nusodinamų dangų spaudimo įtempiai gali sukelti dangų atsiskuoksniovimą nuo pagrindo, o tempimo įtempiai – dangų sutrūkinėjimą. Mokslinėje literatūroje duomenų apie Te junginių priedų elektrolite įtaką Mn elektrolitinių dangų mikrokietumui ir vidiniams įtempiams nėra daug.

Todėl teoriniu ir praktiniu požiūriu ypač aktualu nustatyti Te junginių priedo įtaką elektrolitinių Mn dangų fizikinėms–mechaninėms savybėms, kurios lemia dangų korozines savybes.

Šis darbas yra anksčiau Kauno technologijos universiteto Fizikinės ir neorganinės chemijos katedroje vykdytų Mn ir jo lydinių elektrochemijos tyrimų tęsinys ir skirtas elektrolitinių Mn dangų nusodinimui ir apibūdinimui.

**Darbo tikslas.** Nustatyti Te(VI) priedo amoniakiniame sulfatiniame manganavimo elektrolite įtaką elektrolitinių mangano dangų nusodinimui ir iširti Mn dangų fizikines–mechanines savybes. Įvertinti elektrolitinių Mn dangų, su įsiterpusio Te priemaišomis, pritaikymo galimybes plieno saugai nuo korozijos.

Siekiant darbo tikslo, reikėjo išspręsti **šiuos uždavinius**:

1. Iš stabilaus, optimalios sudėties rūgštaus amoniakinio sulfatinio manganavimo elektrolito, su nedidelėmis Te(VI) priedo koncentracijomis nusodinti elektrolitinio Mn dangas, iširti jų cheminę ir fizinę sudėtį, srovinę išėigą, dangų morfologiją, fizikines–mechanines savybes ir atsparumą korozijai.

2. Iširti 0,55–2,20 mmol/l Te(VI) priedo koncentracijos ir temperatūros įtaką Mn elektronusodinimo procesui ir katodo poliarizacijai rūgščiame amoniakiniame sulfatiniame manganavimo elektrolite.

3. Iširti elektrolitinių Mn dangų, turinčių Te, įtaką koroziniam atsparumui ir įvertinti fosfatinių dangų įtaką atsparumui.

**Mokslinis naujumas.**

1. Nustatytos optimalios elektrolizės sąlygos, leidžiančios nusodinti nanokristalines, atsparias korozijai Mn dangas, turinčias Te, iš rūgštaus amoniakinio sulfatinio manganavimo elektrolito. Nustatytas fosfatinių dangų įtakos elektrolitinių mangano dangų, turinčių Te, atsparumo korozijai ryškus padidėjimas.

2. Nustatyta elektrolito temperatūros ir srovės tankio įtaka elektrolitinių Mn dangų, nusodintų iš ASME su Te(VI) priedu, morfologijai, kristalitų dydžiui, vidiniams įtempiams ir mikrokietaumui.

3. Nustatyta, kad amoniakiniame sulfatiniame manganavimo elektrolite elektrolitinio Mn dangos yra nanokristalinės, o vidutinis kristalitų dydis ir Te koncentracijos pokyčiai dangų paviršiaus įdubose ir iškilimuose priklauso nuo srovės tankio ir elektrolito temperatūros.

**Praktinė vertė.** Optimaliomis elektrolizės sąlygomis (2,2 mmol/l Te(VI) priedo koncentracija, srovės tankis 15 A/dm<sup>2</sup>) iš rūgštaus amoniakinio sulfatinio manganavimo elektrolito nusodintos nanokristalinės elektrolitinio Mn dangos, turinčios Te, gali būti naudojamos plieno antikoroziinei apsaugai.

**Darbo aprobavimas ir publikavimas.** Disertacijos tema yra paskelbta 8 publikacijose: 3 straipsniai žurnaluose, įtrauktuose į Mokslinės informacijos instituto (ISI) duomenų bazę, 2 žurnale „Cheminė technologija“ ir 3 pranešimai konferencijų medžiagoje.

**Darbo apimtis.** Disertaciją sudaro įvadas, literatūros apžvalga, naudotos medžiagos ir tyrimų metodika, rezultatai ir jų aptarimas, išvados, publikacijų disertacijos tema sąrašas. Pateikiamas 128 šaltinių sąrašas. Pagrindinė medžiaga išdėstyta 87 puslapiuose, įskaitant 48 paveikslėlius ir 17 lentelių.

### **Ginamieji disertacijos teiginiai.**

1. Rūgščiajame elektrolite katodo paviršiuje susidaręs elementinis Te depoliarizuoja katodinį procesą ir lemia tolesnę didesnę vertės ribinės srovės atsiradimą potencialų nuo -1,1 V iki -1,3 V intervale. Įrodyta, kad šių potencialų intervale anginio plieno katodo paviršiuje susidaro atskiri MnTe kristalaitai.

2. Nusodintos amoniakiniame sulfatiniame manganavimo elektrolite elektrolitinio Mn dangos yra nanokristalinės, o dangų paviršiuje esančiose įdubose ir iškilimuose Mn ir Te koncentracijos kinta atsižvelgiant į elektrolizės sąlygas.

3. Elektrolitinės Mn dangos, turinčios Te, nusodintos esant 15 A/dm<sup>2</sup>, yra atsparios korozijai. Naudojant fosfatines dangas elektrolitinių Te turinčių mangano dangų atsparumas korozijai padidėja.

### **IŠVADOS**

1. Elektrolitinės Mn dangos, turinčios Te, nusodinamos iš stabilaus rūgštaus amoniakinio sulfatinio manganavimo elektrolito (0,95 mol/l (NH<sub>4</sub>)<sub>2</sub>SO<sub>4</sub>, 0,62 mol/l MnSO<sub>4</sub>·5H<sub>2</sub>O, pH = 2,3, kaip Te(VI) priedas natrio telūratas Na<sub>2</sub>TeO<sub>4</sub>·2H<sub>2</sub>O).

2. Katodo paviršiuje susidaręs elementinis Te depoliarizuoja katodinį procesą ir lemia tolesnę didesnės vertės ribinės srovės atsiradimą potencialų nuo -1,1 V iki -1,3 V intervale. Įrodyta, kad anglinio plieno katodo paviršiuje šių potencialų intervale susidaro atskiri MnTe kristalitai.

3. Pradinėje elektrolizės stadijoje į Mn dangas įsiterpęs Te turi įtakos dangų struktūrai ir morfologijai. Nusodinant elektrolitines Mn dangas esant  $i_k = 2\text{--}10 \text{ A/dm}^2$ , nustatyta, kad jas sudaro dviejų atmainų mišinys: kietoji  $\alpha\text{-Mn}$  ir plastiškoji  $\beta\text{-Mn}$ . Esant didesniems srovės tankiams Mn dangose nustatyti žymesni struktūriniai pokyčiai.

4. Didinant elektrolito temperatūrą nuo 20 °C iki 80 °C, kinta dangų struktūra: iš  $\alpha\text{-Mn}$  ir  $\beta\text{-Mn}$  atmainų mišinio į  $\alpha\text{-Mn}$  atmainą. Elektrolito temperatūros didinimas elektrolitinių Mn dangų srovinę išeią padidina nuo 37 iki 71 % ( $i_k = 15 \text{ A/dm}^2$ ), o Te koncentraciją nuo 0,9 iki 1,6 %.

5. Elektrolitinės Mn dangos, nusodintos iš elektrolito, esant 2–30 A/dm<sup>2</sup> srovės tankiui ir 2,20 mmol/l Te(VI) priedo, yra nanokristalinės. Vidutinis kristalitų dydis, didinant srovės tankį sumažėja nuo 75 nm iki 18–26 nm. Didinant elektrolito temperatūrą nuo 20 iki 80 °C vidutinis kristalitų dydis mažėja nuo 25 iki 15 nm ( $i_k = 15 \text{ A/dm}^2$ ).

6. Nepriklausomai nuo Te(VI) priedo koncentracijos elektrolite, Te koncentracija Mn dangų paviršiaus įdubose yra didesnė nei iškilimuose. Tačiau didėjant Te(VI) priedo koncentracijai ASME šis skirtumas mažėja. Didžiausi Te koncentracijos skirtumai yra 20 °C temperatūroje. Pastarieji, didinant elektrolito temperatūrą nuo 20 iki 80 °C mažėja.

7. Elektrolitinėms Mn dangoms, nusodintoms iš 20 °C temperatūros elektrolito, būdingi dideli tempimo vidiniai įtempiai. Mažiausi tempimo vidiniai įtempiai ( $\sigma \sim 22 \text{ MPa}$ ) nustatyti kai  $i_k = 2 \text{ A/dm}^2$ , o didžiausi ( $\sigma \sim 91 \text{ MPa}$ ) kai  $i_k = 10\text{--}15 \text{ A/dm}^2$ .

8. Įsiterpęs į elektrolitines Mn dangas, Te turi įtakos dangų mikrokietumui. Didinant srovės tankį Mn dangų mikrokietumas sumažėja atitinkamai nuo 2721,6±32,6 iki 1820,2±11,96 MPa, o didinant elektrolito temperatūrą geriausios kokybės Mn dangų mikrokietumas mažėja nuo 1820,2±11,96 iki 1452,3±17,4 MPa.

9. Remiantis Mn dangų korozijos kinetiniais parametrais ir tyrimais druskos rūko kameroje nustatyta, kad atspariausios korozijai Mn dangos, turinčios Te, nusodinamos esant 15 A/dm<sup>2</sup> srovės tankiui. Dangų atsparumas labai padidėja jas padengus fosfatų plėvele.

UDK 544.654.2 (043.3)

SL 344. 2015-11-09, 2,25 leidyb. apsk. I. Tiražas 50 egz. Užsakymas 399.

Išleido Kauno technologijos universitetas, K. Donelaičio g. 73, 44249 Kaunas  
Spausdino leidyklos „Technologija“ spaustuvė“, Studentų g. 54, 51424 Kaunas